Interactions between Cytochrome c_2 and the Photosynthetic Reaction Center from *Rhodobacter sphaeroides*: The Cation−π Interaction†

M. L. Paddock, K. H. Weber, C. Chang, and M. Y. Okamura*

Department of Physics, University of California at San Diego, 9500 Gilman Drive, La Jolla, California 92093

Received April 8, 2005; Revised Manuscript Received May 18, 2005

ABSTRACT: The cation−π interaction between positively charged and aromatic groups is a common feature of many proteins and protein complexes. The structure of the complex between cytochrome c_2 (cyt c_2) and the photosynthetic reaction center (RC) from *Rhodobacter sphaeroides* exhibits a cation−π complex formed between Arg-C32 on cyt c_2 and Tyr-M295 on the RC [Axelrod, H. L., et al. (2002) *J. Mol. Biol. 319*, 501−515]. The importance of the cation−π interaction for binding and electron transfer was studied by mutating Tyr-M295 and Arg-C32. The first- and second-order rates for electron transfer were not affected by mutating Tyr-M295 to Ala, indicating that the cation−π complex does not greatly affect the association process or structure of the state active in electron transfer. The dissociation constant K_D showed a greater increase when Try-M295 was replaced with nonaromatic Ala (3-fold) as opposed to aromatic Phe (1.2-fold), which is characteristic of a cation−π interaction. Replacement of Arg-C32 with Ala increased K_D (80-fold) largely due to removal of electrostatic interactions with negatively charged residues on the RC. Replacement with Lys increased K_D (6-fold), indicating that Lys does not form a cation−π complex. This specificity for Arg may be due to a solvation effect. Double mutant analysis indicates an interaction energy between Tyr-M295 and Arg-C32 of approximately −24 meV (−0.6 kcal/mol). This energy is surprisingly small considering the widespread occurrence of cation−π complexes and may be due to the tradeoff between the favorable cation−π binding energy and the unfavorable desolvation energy needed to bury Arg-C32 in the short-range contact region between the two proteins.

Noncovalent molecular interactions play an important role in molecular association processes in biological systems (*1*−*3*). Among these interactions are hydrogen bonds, hydrophobic interactions, and ion-paired salt bridges (*2*, *3*). In addition to these, the cation−π interaction, the short-range electrostatic interaction between a positively charged cation and π electrons in an aromatic group (*4*), has been found to play a role in biological systems. The cation−π interaction is important in ligand binding (*5*), in protein structures (*6*), and in protein−protein complexes (*7*). This work concerns a cation−π interaction found in the interface between the cytochrome c_2 (cyt c_2)[1] and the reaction center (RC) of *Rhodobacter* (*Rb.*) *sphaeroides* that is formed between Arg-C32 on the cyt c_2 and Tyr-M295 on the RC (*8*). The importance of this cation−π interaction with respect to the binding and electron transfer reactions between the two proteins was studied by site-directed mutation of both Arg-C32 on the cyt c_2 and Tyr-M295 on the RC.

The RC (*9*, *10*) is a membrane-bound pigment−protein complex in photosynthetic bacteria that performs the initial light-induced electron transfer reactions to convert sunlight into chemical energy (*11*). Light absorbed by the RC induces electron transfer from a special bacteriochlorophyll dimer, D, the primary donor, through a series of bound electron acceptors to a bound ubiquinone (Q_B). The photo-oxidized donor (D^+) is reduced by electron transfer from a water soluble cyt c_2, allowing electrons to flow through a membrane-associated electron transfer chain in a cycle that is coupled to proton pumping that drives ATP synthesis. Operation of the photocycle relies on efficient reactions between the mobile cyt c_2 and the membrane-bound RC. For efficient operation, cyt c_2 must associate with the RC, transfer electrons, and dissociate within the time scale of electron turnover in the cycle ($\sim 10^{-3}$ s) (*12*).

The binding and electron transfer rates of isolated cyt c_2 and the RC have been extensively studied using laser pulse kinetic measurements (*13*−*18*). The reduction of oxidized donor D^+ by reduced cyt c_2 shows two kinetic phases following a single laser flash: a fast (microsecond) first-order phase (independent of cyt c_2 concentration) due to electron transfer from bound cyt c_2 to the photo-oxidized donor of the RC and a slower (millisecond) second-order phase (dependent on cyt c_2 concentration) due to the binding and subsequent electron transfer of free cyt c_2. The observed biphasic kinetics can be explained by the following scheme (*17*).

$$\begin{array}{ccc} \text{cyt } c_2^{2+} + DQ_B & \overset{K_D}{\leftrightarrow} & \text{cyt } c_2^{2+} : DQ_B \\ & & \downarrow h\nu \\ \text{cyt } c_2^{2+} + D^+Q_B^- & \underset{k_{off}}{\overset{k_{on}}{\rightleftharpoons}} & \text{cyt } c_2^{2+} : D^+Q_B^- \xrightarrow{k_e} \text{cyt } c_2^{3+} : DQ_B^- \end{array} \quad (1)$$

where K_D is the dissociation constant, k_{on} is the association

† This work was supported by NIH Grant GM 41637.

* To whom correspondence should be addressed. Phone: (858) 534-2506. Fax: (858) 822-0007. E-mail: mokamura@ucsd.edu.

[1] Abbreviations: cyt c_2, cytochrome c_2; RC, reaction center; cyt bc_1, cytochrome bc_1; Q_{10}, ubiquinol-10; D, primary electron donor (bacteriochlorophyll dimer); D^+, photo-oxidized primary electron donor; Q_B, bound acceptor quinone; k_e, first-order electron transfer rate; k_2, observed second-order rate constant; K_D, dissociation constant; Q_0, 2,3-dimethoxy-5-methyl-1,4-benzoquinone.

10.1021/bi050651d CCC: $30.25
Published on Web 06/18/2005

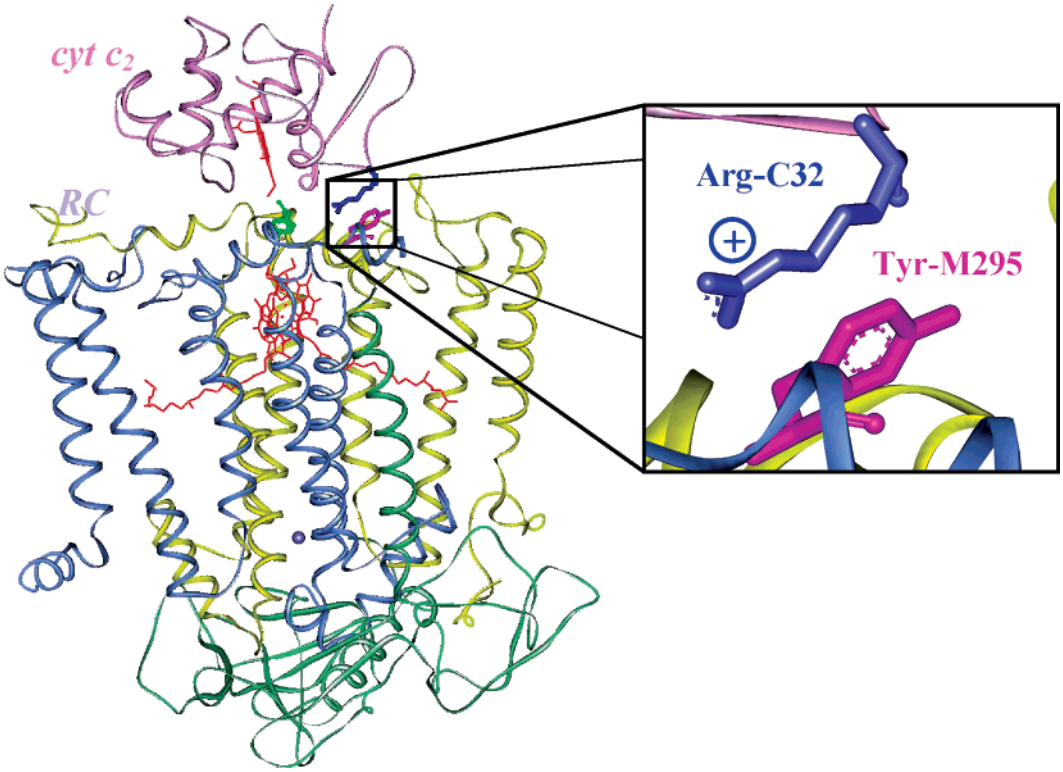

FIGURE 1: Cation−π interaction in the RC−cyt c_2 complex [PDB entry 1L9B (*8*)]. RC subunits L, M, and H are colored yellow, blue, and green, respectively. The primary donor (bacteriochlorophyll dimer) of the RC is colored red. The cyt c_2 colored lavender binds with its heme cofactor (red) just above the primary RC donor. Tyr-L162, in contact with both cofactors, is colored green. Arg-C32 (blue) of cyt c_2 and Tyr-M295 (purple) of the RC form a cation−π interaction in the docked complex. This interaction is enlarged in the box at the right; the view was slightly changed to better emphasize the interaction.

rate constant, k_{off} is the dissociation rate constant, and k_e is the electron transfer rate constant in the bound state. The equilibrium between bound and free cyt c_2 is achieved in the dark. Following a laser flash, the re-reduction of D^+ by cyt c_2^{2+} is biphasic. RCs with a bound cyt c_2 undergo rapid electron transfer with a rate constant k_e ($\approx 10^6$ s^{-1}) (*14*). RCs without a bound cyt c_2 undergo slower diffusion-limited electron transfer with an observed second-order rate constant k_2 ($\sim 10^9$ s^{-1} M^{-1}) (*18*). Since $k_e \gg k_{off}$ (*19*), the observed second-order rate constant is the association rate ($k_2 \sim k_{on}$) (*20*). The fraction of RCs with a bound cyt c_2 can be determined by the ratio of the fast and slow phases. The dissociation constant K_D can be determined from a plot of the fraction of RCs with bound cyt c_2 versus the free cyt c_2 concentration. The importance of electrostatic interactions for binding and electron transfers between cyt c_2 and the RC has been established by the ionic strength dependence of k_2 (*13*), the effect of site-directed mutation of charged residues (*17*, *21*), chemical cross-linking (*22*−*24*), and electrostatic modeling (*15*, *25*, *26*). Hydrophobic interactions, particularly those of Tyr-L162 on the RC, have been shown to be important for binding and electron transfer (*18*, *27*).

The structure of the cyt c_2−RC complex was obtained by cocrystallizing the two proteins in a photochemically active complex and determining its X-ray crystal structure (*8*). The structure of the complex shows the binding site to be between the cyt c_2 and the periplasmic surface of the RC with a central short-range contact region in which the exposed heme edge is in contact with Tyr-L162, directly above the BChl dimer (Figure 1). The close contact between the two proteins provides an efficient tunneling pathway for fast electron transfer in the bound state. In the central region, the residues from the two proteins make contact through van der Waals and hydrogen bonding interactions as well as the cation−π interaction (Figure 1). The shortest distance between the positively charged guanidinium group of Arg-C32 and the phenolic group of Tyr-M295 is less than 4 Å, characteristic of a cation−π complex (*6*). Surrounding the central region of close contact is a solvent-separated region having positively charged residues on the cyt c_2 positioned opposite negatively charged residues on the RC interface between the two proteins. The charged residues do not form salt bridges but are separated by solvent.

In this work, the functional role of the cation−π interaction in the binding, association, and electron transfer between cyt c_2^{2+} and the RC is addressed to answer the following questions. (1) What is the magnitude of this interaction? (2) Is this interaction important for the association of cyt c_2 and the RC? (3) Is it important for interprotein electron transfer? To answer these questions, site-directed mutants of the RC (at Tyr-M295) and cyt c_2 (at Arg-C32) were constructed. Mutants were created that replaced aromatic residue Tyr-M295 on the RC with either aromatic or nonaromatic residues and replaced cationic residue Arg-C32 on cyt c_2 with either the cationic Lys residue or neutral residues. The effects of these mutations on binding and electron transfer rates were measured by transient absorption spectroscopy using flash photolysis and compared to native values.

MATERIALS AND METHODS

Site-Directed Mutagenesis. The site-directed mutations on the RC were constructed as previously described using the

QuickChange mutagenesis kit (Stratagene) and a Perkin-Elmer PCR system (*28*). The site-directed mutation on the cyt c_2 gene were constructed as follows. First, *cycA*, the gene encoding the cyt c_2 protein, was transferred on a 2.7 kb *Pst*I fragment from pC2P404.1 (*18*) to pBCSK(+) (Stratagene, La Jolla, CA), creating pBC*cycA*. Mutations were introduced into the plasmid via the QuickChange mutagenesis kit as discussed above. The mutation was confirmed by DNA sequencing [University of California at San Diego (UCSD) Molecular Pathology Shared Resource in the UCSD Cancer Center]. The *Pst*I fragment carrying *cyc A* was transferred into pRK404, creating pRKcycA*. pRKcycA* was transformed into S17-1 and conjugated into CYCA1, the *Rb. sphaeroides* host lacking *cyc A* (*29*), for transcription and translation of the modified gene sequence.

Protein Isolation and Purification. The bacteria harboring the modified RC or cyt c_2 gene were grown in the dark as described previously (*28*). RCs from *Rb. sphaeroides* carotenoidless strain R26 (native) and mutant strains were isolated in 15 mM Tris-HCl (pH 8), 0.025% lauryl dimethylamine *N*-oxide (LDAO), and 0.1 mM EDTA following published procedures (*28*). The final ratio of absorbance (A_{280}/A_{800}) was $\leq$1.5. The RC samples were then dialyzed for 2 days against HM [10 mM Hepes (pH 7.5) and 0.04% dodecyl β-D-maltoside (Anatrace)].

Native and mutant cyt c_2 proteins were isolated and purified as previously reported (*30*). Samples were purified to an A_{280}/A_{412} absorbance ratio of $\leq$0.3. Mass spectroscopy was performed (UCSD Department of Chemistry, mass spectrometry facility) to verify the Arg-C32 $\rightarrow$ Gln and Arg-C32 $\rightarrow$ Lys substitutions in the mutant cyt c_2 proteins.

Quinone/Quinol Preparations. Quinone (Q_0) (2,3-dimethoxy-5-methylbenzoquinone) was obtained from Aldrich in $\geq$99% purity. Quinol (Q_0H_2) was synthesized by reducing quinone with hydrogen gas in the presence of platinum black, which was also obtained from Aldrich.

Electron Transfer Measurements. The kinetics of electron transfer between the RC and cyt c_2 were measured by flash absorption spectroscopy as described previously (*31*). Absorbance changes were measured at 865 or 595 nm following a laser flash from a Nd:YAG laser with a tunable optical parametric oscillator (Opotek, $\lambda = 800$ nm, $\tau = 10$ ns). All measurements were conducted at 23 °C in a buffer of 10 mM Hepes and 0.04% β-maltoside at pH 7.5. Samples included 50 μM Q_0 and Q_0H_2 to ensure that the cyt c_2 was reduced prior to each laser flash.

The fraction of RC with and without a bound cyt ${c_2}^{2+}$ were determined from the relative amplitudes of the fast and slow phases of the reduction of D^+ by the cyt ${c_2}^{2+}$. The concentration of free cyt ${c_2}^{2+}$ was obtained by subtracting the concentration of bound cyt ${c_2}^{2+}$ from the total concentration that had been added. The value of the dissociation constant (K_D) was determined from the dependence of the fraction bound on the concentration of free cyt ${c_2}^{2+}$. The change in free energy due to mutation of residue *i* was obtained from the following relation as described in ref *18*:

$$\Delta\Delta G_i = RT \ln\frac{K_{D,i}}{K_{D,0}} \quad (2)$$

where $K_{D,i}$ and $K_{D,0}$ are the dissociation constants for mutant and native complexes, respectively. The second-order rate constant (k_2) was determined from the concentration dependence of the measured rate constant for the slow phase of D^+ re-reduction. When the concentration of cyt c_2 is large compared to that of the RC, the reaction becomes pseudo-first-order in cyt c_2. To maximize the concentration range over which this condition holds, the RC concentration was kept low (0.2 μM). The first-order electron transfer rate constants (k_e) were measured at 595 nm with a higher RC concentration (5 μM RC and 30 μM cyt c_2). With no cyt c_2 present, some mutant RCs produced a small transient signal at this wavelength, which was subtracted from the observed kinetic trace.

Determination of the Cation−π Interaction Energy by Double Mutant Analysis. The specific cation−π interaction energy can be estimated by double mutant analysis of changes due to mutation of Arg-C32 and Tyr-M295. The relation of the changes in free energy due to mutation and the cation−π interaction energy is illustrated by the double mutant cycle (*31*−*33*). The interaction energy between two residues can be estimated by the interaction energy $\Delta\Delta G_{int}$

$$\Delta\Delta G_{int} = \Delta\Delta G_{YR} - \Delta\Delta G_Y - \Delta\Delta G_R = -RT \ln\frac{K_{D,Y}K_{D,R}}{K_{D,0}K_{D,YR}} \quad (3)$$

where $\Delta\Delta G_Y$ and $\Delta\Delta G_R$ are the changes in free energy obtained for the binding reactions of RCs modified at Tyr-M295 to native cyt c_2 and cyt c_2 modified at Arg-C32 with native RCs, respectively, and $\Delta\Delta G_{YR}$ is the change in free energy for the binding between the modified RC and modified cyt c_2. $K_{D,Y}$, $K_{D,R}$, and $K_{D,YR}$ are the corresponding changes in the dissociation constant. $K_{D,0}$ is the dissociation constant of native cyt c_2 and RC.

The change in free energy due to mutation of Tyr-M295 is assumed to be due to contributions from the cation−π interaction of Tyr-M295 with Arg-C32 ($\Delta\Delta G_{cat-\pi}$) and nonspecific interactions with other residues ($\Delta\Delta G_{YX}$).

$$\Delta\Delta G_Y = \Delta\Delta G_{cat-\pi} + \Delta\Delta G_{YX} \quad (4)$$

The major contributions to $\Delta\Delta G_{cat-\pi}$ are the increase in free energy due to the loss of the cation−π interaction and the decrease due to the loss of the solvation penalty; it will also include changes in other specific interactions between the two residues such as those due to van der Waals contacts. These cannot be separated in this analysis.

The change in binding free energy due to mutation of Arg-C32 ($\Delta\Delta G_R$) is assumed to have contributions from $\Delta\Delta G_{cat-\pi}$ between Arg-C32 and Tyr-M295 and interactions between Arg-C32 and other residues on the RC ($\Delta\Delta G_{RX}$). In addition, we specifically include an additional term $\Delta\Delta G_{elect}$, which is due to the electrostatic interaction of positively charged Arg-C32 with the negative potential of the RC surface that is lost due to mutation to a neutral residue X.

$$\Delta\Delta G_R = \Delta\Delta G_{cat-\pi} + \Delta\Delta G_{elect} + \Delta\Delta G_{RX} \quad (5)$$

The change in free energy due to the mutation of the two interacting residues ($\Delta\Delta G_{RY}$) can be expressed as

$$\Delta\Delta G_{RY} = \Delta\Delta G_{cat-\pi} + \Delta\Delta G_{elect} + \Delta\Delta G_{RX} + \Delta\Delta G_{YX} \quad (6)$$

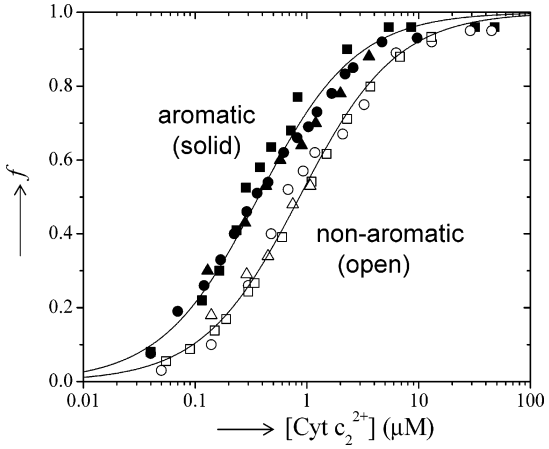

FIGURE 2: Binding data for the native cyt c_2 with the native and mutant RCs. Shown is a plot of *f*, the fraction of RC with a bound cyt c_2, vs the concentration of free cyt c_2^{2+}. Data for binding of cyt c_2 to RCs with an aromatic residue at position M295 are shown as filled symbols [native (■), Tyr → Phe (●), and Tyr → Trp (▲)]. Data for binding of cyt c_2 to RCs without an aromatic residue are shown as empty symbols [Tyr → Leu (□), Tyr → Asn (○), and Tyr → Ala (△)]. The solid lines are the binding curves using the average value of K_D for the aromatic (0.34 μM) and nonaromatic (0.86 μM) mutant RCs. Note that K_D values for all of the aromatic residues at position M295 are within error indistinguishable. Similarly, K_D values for all of the nonaromatic substitutions are within error indistinguishable, but differ by ~3-fold from the native value. Conditions: 10 mM Hepes (pH 7.5), 0.04% β-maltoside, 50 μM Q_0, and 50 μM Q_0H_2.

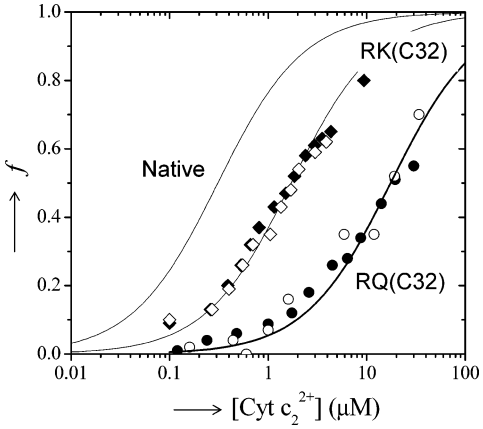

FIGURE 3: Binding data for cyt c_2 mutants that lack the cationic Arg-C32 with the native and mutant RCs lacking the π system at position M295. Diamonds represent data for the mutation of Arg-C32 to Lys, and circles represent data for the mutation of Arg-C32 to Gln. Filled symbols are for binding of the mutant cyt c_2 to the native RC. Empty symbols are for binding of the mutant cyt c_2 to the Tyr-M295 → Leu mutant RC. The binding curve for the native system is shown for reference. Note that the binding of the mutant cyt c_2 is essentially the same to either the native or mutant RC, indicating that the mutations introduce little if any secondary change that affects the binding. Conditions were those described in the legend of Figure 2.

where it is assumed that the interactions changed by single mutations are the same in the double mutation; i.e., the structure of the complex containing single mutations is the same (apart from the local changes to the mutated residue) as that containing both mutations. From eqs 3−6, the interaction free energy between the mutated residues is the negative of the free energy increase due to loss of the cation−π interaction.

$$\Delta\Delta G_{int} = -\Delta\Delta G_{cat-\pi} \quad (7)$$

Thus, the cation−π interaction energy can be obtained from double mutant analysis.

RESULTS

Dissociation Constants (K_D). K_D and $\Delta\Delta G$ values were obtained from the dependence of the fraction of the RC with a bound cyt c_2 on the free concentration of cyt c_2. The binding curves are presented in Figures 2 and 3, and the results are summarized in Table 1.

Reaction Center Mutations. Mutation of Tyr-M295 on the RC to aromatic residues Phe and Trp had small effects on K_D (increases by factors of 1.3 and 1.5, respectively), indicating that these aromatic residues can also participate in a cation−π interaction with Arg-C32. Mutation of Tyr-M295 to Asn, Leu, and Ala produced larger changes in K_D (up to a factor of 3). The changes in free energy due to these mutations increased up to a maximum $\Delta\Delta G$ of 28 meV for Tyr-M295 to Leu and Ala mutations. The free energy changes can be attributed largely to the loss of the cation−π interaction.

Cytochrome Mutations. Mutation of Arg-C32 to Lys, Gln, and Ala increased K_D by factors of 5.6, 50, and 80. These changes were larger than those produced by mutation of Tyr-M295. The larger changes in free energy (100 and 112 meV) due to the mutation of the cationic Arg to neutral Gln and Ala, respectively, result from the additional loss of stabilizing electrostatic interaction between Arg and the negative potential due to acidic residues on the RC surface (*17*).

Table 1: Binding and Electron Transfer Parameters for Single and Double Mutant Reactions of RCs Modified at Tyr-M295 and Cyt c_2 Modified at Arg-C32 (pH 7.5)[a]

RC strain	cyt c_2	k_e ($\times 10^6$ s^{-1})	k_2 ($\times 10^8$ M^{-1} s^{-1})	K_D (μM)	$\Delta\Delta G$ (meV)
native	native	1.0	13.1	0.30	0
Tyr-M295 → Phe	native	1.1	13.4	0.38	6
Tyr-M295 → Trp	native	0.9	12.5	0.44	10
Tyr-M295 → Asn	native	1.0	13.2	0.78	24
Tyr-M295 → Leu	native	0.9	13.1	0.89	28
Tyr-M295 → Ala	native	1.0	12.1	0.91	28
native	Arg-C32 → Lys	0.9	4.6	1.7	44
native	Arg-C32 → Gln	0.6	7.8	15	100
native	Arg-C32 → Ala	0.8	6.1	24	112
Tyr-M295 → Leu	Arg-C32 → Lys	0.9	3.4	1.8	46
Tyr-M295 → Leu	Arg-C32 → Gln	0.6	7.1	17	103
Tyr-M295 → Ala	Arg-C32 → Ala	0.7	6.7	31	118

[a] k_e is the rate constant for the fast, first-order electron transfer. k_2 is the second-order rate constant. K_D is the dissociation constant for the cyt c_2−RC complex. $\Delta\Delta G = RT \ln(K_{D,i}/K_{D,0})$, which is the difference in binding free energy between the mutant and native RCs. The experimental precision for the measured values of the rates and K_D is ±15%. The uncertainty in the free energies is ±5 meV.

Second-Order Association Rate Constants (k_2). Second-order rate constants were obtained from plots of the observed kinetic rate against the concentration of free cyt c_2 (*17*, *31*). Mutant RCs had the same second-order rate constant within experimental error ($k_2 = 12-13 \times 10^8$ M^{-1} s^{-1}) as the native RC for the native cyt c_2. The mutations to cyt c_2 (Arg-C32 → Lys, Arg-C32 → Gln, and Arg-C32 → Ala) resulted in smaller values of k_2 (5×10^8, 8×10^8, and 6×10^8 M^{-1} s^{-1}, respectively) that accompanied the increase in dissociation constant K_D.

First-Order Electron Transfer Rate Constants (k_e). The first-order electron transfer rate constant for the native RC−cyt c_2 system was found to be 1×10^6 s^{-1}, as previously reported (*14*−*18*). All mutant RCs bound with native cyt c_2 had the same first-order rate constant ($k_e = 0.9-1.1 \times 10^6$ s^{-1}). Similarly, $k_e = 0.9 \times 10^6$ s^{-1} for electron transfer between the bound Arg-C32 → Lys mutant cyt c_2 and the native RC. Small changes were observed in k_e for electron transfer between the native RC and the Arg-C32 → Gln cyt c_2 ($k_e = 0.6 \times 10^6$ s^{-1}) or the Arg-C32 → Ala cyt c_2 ($k_e = 0.8 \times 10^6$ s^{-1}).

DISCUSSION

Role of the Cation−π Interaction in Binding. The mutation of either the cationic or the aromatic partner in the cation−π complex resulted in changes in the binding of the cyt c_2 to the RC. Replacement of Tyr-M295 with Ala, Asn, or Leu lacking π electrons had the effect of increasing K_D (by up to 3-fold for Ala), while replacement of Tyr-M295 with the other aromatic residues, Phe and Trp, had a relatively small effect. These results are characteristic of the formation of a cation−π complex at the cyt c_2−RC interface and indicate that an aromatic residue at position M295 assists the binding of the cyt c_2 to the RC. The removal of the cationic Arg-C32 residue and replacement with neutral residues Ala and Gln resulted in a larger increase in K_D (by up to 80-fold), corresponding to a change in the binding free energy of ∼110 meV. The larger effect upon mutation of the cationic residue can be attributed to the loss of the electrostatic interactions between Arg-C32 and residues other than Tyr-M295. The strongest interaction is likely to be the electrostatic interaction between Arg-C32 and Asp-L155 at a distance of 7 Å (*8*). The Coulombic interaction between the two charged residues would have an energy of ∼100 meV at that distance, for a dielectric constant of 20.

The double mutant cycle provides a means of assessing the magnitude of the cation−π interaction energy between the two mutated residues. From the three double mutant cycles involving mutations in this study (Arg-C32 → Lys and Tyr-M295 → Leu, Arg-C32 → Gln and Tyr-M295 → Leu, and Arg-C32 → Ala and Tyr-M295 → Ala), $\Delta\Delta G_{int}$ values of −26, −25, and −22 meV, respectively, were obtained from eq 3, giving an average of −24 ± 2 meV. The values obtained for all three mutant cycles are in good agreement with each other. The cation−π interaction energy is close to the magnitude of the free energy change for mutation of Tyr-M295 to Ala, indicating that the interactions of Tyr-M295 with residues besides Arg-C32 are weak ($\Delta\Delta G_{YX} \sim 4$ meV, eq 4)

The specific site−site interaction between Arg-C32 and Tyr-M295 has a relatively small net contribution to the binding free energy of the complex [$\Delta\Delta G_{int} = -24$ meV (−0.6 kcal/mol ∼ k_BT)]. The cation−π interaction between Arg-C32 and Tyr-M295 in the cyt c_2−RC complex was identified by CAPTURE (*6*) (http://capture.caltech.edu/) that has been successfully used to identify cation−π interactions in many other protein structures. Gas phase estimates of the electrostatic and van der Waals contributions were computed to be approximately −4 kcal/mol (−170 meV) and approximately −2 kcal/mol (−85 meV), respectively [average of three structures in two crystal forms (PDB entries 1L9B and 1L9J)]. Note that these values are much larger than the smaller observed net effect which includes the competing energy cost required to desolvate the cation. Since the guanidinium group is positively charged, it interacts with water dipoles and forms hydrogen bonds. Upon formation of the cyt c_2−RC complex, Arg-C32 becomes largely inaccessible to solvent. The solvent accessibility for the Arg-C32 side chain changes from 55 to 3% upon formation of the cyt c_2−RC complex [determined using CNS (*34*)]. Thus, significant energy is required to desolvate the cationic guanidinium group to bring it into close contact with the Tyr.

Although Lys is capable of participating in a cation−π interaction, the change in the interaction energy between Lys-C32 and Tyr-M295 ($\Delta\Delta G_{int} = -26$ meV from the double mutant analysis) suggests that Lys-C32 does not form a cation−π complex. The change in free energy ($\Delta\Delta G_R$) of 44 meV for mutation of the charged Arg-C32 to Lys which is larger than those found for the mutations of aromatic Tyr-M295 to either Leu or Ala could be due to changes in the electrostatic interaction due to the Arg → Lys mutation; i.e., $\Delta\Delta G_{elect}$ in eq 5 is not zero. This change could result from a difference in the Coulombic interaction, due to a change in the position of the charge on the potential surface or due to a difference in the solvation of Lys and Arg.

The energy cost to desolvate Lys is larger than Arg due to the higher charge density for the ammonium cation than the guanidinium cation that has charge delocalized over three N atoms. The delocalized charge lowers the desolvation energy compared to that with Lys, making the formation of the cation−π complex with Arg more favorable (*34*). In addition, steric effects may also contribute. The aromatic ring of Tyr-M295 makes the closest contact with the ϵ-nitrogen atom of Arg-C32. The ζ-nitrogen atom of Lys-C32 is one bond length longer and may not be able to form a strong cation−π bond. Crowley and Golovin (*7*) have recently examined a structural database for protein structures having cation−π interactions. They found that the most common cation−π interaction in protein complexes was between Arg and Tyr, with interactions between Lys and Tyr being much less frequent. It is interesting to note that Arg-C32 is the only Arg residue in the interface region, compared to five Lys residues. This suggests that Arg-C32 is selected for its ability to form a cation−π complex in close association with the RC surface.

Role of the Cation−π Interaction in Electron Transfer. The first-order electron transfer rate constants (k_e) for all mutated RCs in this study were very similar to that of native RCs ($k_e = 1.0 \times 10^6$ s^{-1}) (Table 1). Since the first-order rate is due to electron transfer from cyt c_2 in its bound state on the RC surface, we conclude that the positioning of the cyt c_2 on the RC surface is the same with or without the cation−π interaction. Small changes in rate were observed for reaction of the mutant cyt c_2 ($k_e = 0.6-0.9 \times 10^6$ s^{-1}), which could be due to small changes in the redox potential of the mutant cyt c_2, the reorganization energy for electron transfer, or the distance (<1 Å) between the cofactors in the bound state (*36*−*38*).

These results can be rationalized with results from previous experiments using a model in which the electron transfer rate k_e is determined by the close juxtaposition of the exposed heme edge with the short-range contact region on the RC

centered around Tyr-L162 which is in close contact with $BChl_2$ (D) (*8*). Mutation of hydrophobic residues (particularly Tyr-L162) changed the electron transfer rate k_e presumably due to changes in the distance between cofactors in the structure of the modified cyt c_2−RC complex (*18*). In contrast, mutations of charged residues on the RC, located outside of the short-range contact region, did not change the electron transfer rate k_e, although they modified the binding affinity (*17*). The modification of cation−π contacts appears to have effects on k_e similar to those of the charged mutations even though the cation−π complex is part of the short-range interaction region. This may be because the cation−π complex is at the boundary of the short-range contact region. Thus, changes in the cation−π bonding do not affect the structure in the central region around Tyr-L162 which largely determines the rate of electron transfer (*39*, *40*).

Role of the Cation−π Interaction in Cyt c_2 Association and Dissociation. The measured value for the second-order association rate constant was the same for all of the mutated RCs used in this study ($k_2 = k_{on} = 12-13 \times 10^8$ M^{-1} s^{-1}). Thus, the cation−π interaction does not influence the rate of association. This is reasonable since the cation−π interaction is a short-range interaction between a charged residue and the quadrupole moment of a neutral residue. Thus, the formation of the cation−π complex is not expected to be important for the association process since the position of the cyt in the transition state is displaced by ∼10 Å from its position in the bound state (*17*, *25*, *26*). This is consistent with the finding that mutations of hydrophobic residues on the RC do not appreciably affect k_{on} (*18*).

Although the cation−π interaction does not affect the association rate, it does affect the dissociation rate, k_{off}. Since the loss of the cation−π interaction results in a 2−3-fold increase in K_D (Table 1) but no change in k_{on}, the loss of the cation−π interaction results in a 2−3−fold increase in k_{off} ($K_D = k_{off}/k_{on}$). These changes reflect the slightly tighter binding of cyt c_2 to the RC and an increase in the barrier for dissociation in the presence of the interaction. Thus, the cation−π interaction increases the residence time of the cyt c_2 on the RC surface by ∼3-fold. However, if the binding were made substantially tighter, k_{off} would be correspondingly smaller which would substantially reduce the turnover rate of photosynthetic electron transfer. For example, an increase of 60 meV for the cation−π interaction would result in a 10-fold decrease in k_{off} and an ∼10-fold decrease in the overall turnover rate of electron transfer ($\tau = 25$ ms). Thus, a strongly binding cation−π interaction would have a deleterious effect on the photosynthetic efficiency.

Mutations to charged residue Arg-C32 resulted in decreased association rates ($k_2 = 5-8 \times 10^8$ M^{-1} s^{-1}). These changes can be attributed to changes in electrostatic interactions rather than cation−π interaction. The changes in k_2 are consistent with the changes of k_2 due to mutation of charged residues in the interface (*17*, *21*). It is interesting to note that the Arg-C32 → Lys mutation caused the largest change in k_2, suggesting that the configuration of the two residues is significantly different.

Importance of the Arg-C32−Tyr-M295 Interaction. The magnitude for the cation−π interaction in the cyt c_2−RC complex appears to be surprisingly small considering that such complexes have been found in many other systems (*7*), including the complex between cyt *c* and cyt bc_1 from yeast (*41*). Thus, the cation−π interaction in the cyt c_2−RC complex is just one of many interactions (electrostatic, hydrophobic, and hydrogen bonding) that optimize the protein−protein interface, rather than a dominant component of the binding energy. The widespread occurrence of cation−π complexes may be due to the importance of electrostatic interactions (and thus positively charged residues) in the protein association process (*7*). The cationic Arg-C32 is one of several positively charged residues on the cyt c_2 surface that serve to attract and orient the cyt c_2 on the negatively charged binding surface of the RC from a loosely bound encounter complex. Further short-range docking of the cyt c_2 leads through a transition state to the bound state in which electron transfer occurs (*26*). In the bound state, Arg-C32 is buried in the central short-range contact region of the interface where solvent is excluded. In this solvent-excluded region, the two interfaces are in close contact and optimized for electron transfer. In contrast, the other charged residues in the interface are separated by solvent (*8*). The formation of a cation−π complex provides a means of offsetting the cost of desolvating the charge (*42*), thereby providing a means of burying a positively charged group within the solvent-excluded short-range interaction domain. Although the overall cation−π interaction does not greatly increase the binding affinity, the binding is optimized well by other interactions so that a further increase in affinity is not necessary and might slow the dissociation of the oxidized cyt c_2 and thus slow the overall turnover of the reaction.

ACKNOWLEDGMENT

We thank Ed Abresch, Roger Isaacson, and Larry Gross for technical assistance and helpful discussions, Timothy Donohue for providing the cytochrome c_2 deletion strain, and George Feher for helpful discussions. DNA sequencing was performed by the DNA Sequencing Shared Resource, UCSD Cancer Center, which is funded in part by NCI Cancer Center Support Grant 2 P30 CA23100-18.

REFERENCES

1. Kleanthous, C. (2000) *Protein−protein recognition*, Oxford University Press, Oxford, U.K.
2. Jones, S., and Thornton, J. (2000) in *Protein−protein recognition* (Kleanthous, C., Ed.) pp 33−59, Oxford University Press, New York.
3. Stites, W. (1997) Protein−protein interactions: Interface structure, binding thermodynamics, and mutational analysis, *Chem. Rev. 97*, 1233−1250.
4. Ma, J., and Dougherty, D. (1997) The cation-π interaction, *Chem. Rev. 97*, 1303−1324.
5. Zacharius, N., and Dougherty, D. A. (2002) Cation-π interactions in ligand recognition and catalysis, *Trends Pharm. Sci. 23*, 281−287.
6. Gallivan, J. P., and Dougherty, D. A. (1999) Cation-π interactions in structural biology, *Proc. Natl. Acad. Sci. U.S.A. 96*, 9459−9464.
7. Crowley, P., and Golovin, A. (2005) Cation-π interactions in protein−protein interfaces, *Proteins: Struct., Funct., Bioinf. 59*, 231−239.
8. Axelrod, H. L., Abresch, E. C., Okamura, M. Y., Yeh, A. P., Rees, D. C., and Feher, G. (2002) X-ray structure determination of the cytochrome c_2:reaction center electron transfer complex from *Rhodobacter sphaeroides*, *J. Mol. Biol. 319*, 501−515.
9. Gunner, M. (1991) The reaction center protein from purple bacteria: Structure and function, *Curr. Top. Bioenerg. 16*, 319−367.

10. Feher, G., Allen, J. P., Okamura, M. Y., and Rees, D. C. (1989) Structure and function of bacterial photosynthetic reaction centers, *Nature 339*, 111−116.
11. Blankenship, R. E. (2002) *Molecular mechanisms of photosynthesis*, Blackwell Science, London.
12. Crofts, A. R., and Wraight, C. A. (1983) The electrochemical domain of photosynthesis, *Biochim. Biophys. Acta 726*, 149−185.
13. Prince, R. C., Cogdell, R. J., and Crofts, A. R. (1974) The photooxidation of horse heart cytochrome *c* and native cytochrome c_2 by reaction centres from *Rhodopseudomonas spheroides* R-26, *Biochim. Biophys. Acta 347*, 1−13.
14. Overfield, R. E., Wraight, C. A., and Devault, D. C. (1979) Microsecond photooxidation kinetics of cytochrome c_2 from *Rhodopseudomonas sphaeroides*: In vivo and solution studies, *FEBS Lett. 105*, 137−142.
15. Tiede, D., Vashishta, A., and Gunner, M. (1993) Electron-transfer kinetics and electrostatic properties of the *Rhodobacter sphaeroides* reaction center and soluble c-cytochromes, *Biochemistry 32*, 4515−4531.
16. Moser, C., and Dutton, P. L. (1988) Cytochrome *c* and c_2 binding dynamics and electron transfer with photosynthetic reaction center protein and other integral membrane redox proteins, *Biochemistry 27*, 2450−2461.
17. Tetreault, M., Rongey, S. H., Feher, G., and Okamura, M. (2001) Interaction between cytochrome c_2 and the photosynthetic reaction center from *Rhodobacter sphaeroides:* Effects of charge-modifying mutations on binding and electron transfer, *Biochemistry 40*, 8452−8462.
18. Gong, X., Paddock, M. L., and Okamura, M. (2003) Interactions between cytochrome c_2 and photosynthetic reaction center from *Rhodobacter sphaeroides*: Changes in binding affinity and electron transfer rate due to mutation of interfacial hydrophobic residues are strongly correlated, *Biochemistry 42*, 14492−14500.
19. Gerencser, L., Laczko, G., and Maroti, P. (1999) Unbinding of oxidized cytochrome *c* from photosynthetic reaction center of *Rhodobacter sphaeroides* is the bottleneck of fast turnover, *Biochemistry 38*, 16866−16875.
20. Bendall, D. (1996) in *Protein electron transfer* (Bendall, D., Ed.) pp 43−68, Bios Scientific Publishers Ltd., Oxford, U.K.
21. Caffrey, M. S., Bartsch, R. G., and Cusanovich, M. A. (1992) Study of the cytochrome c_2-reaction center interaction by site-directed mutagenesis, *J. Biol. Chem. 267*, 6317−6321.
22. Rosen, D., Okamura, M. Y., Abresch, E. C., Valkirs, G. E., and Feher, G. (1983) Interaction of cytochrome *c* with reaction centers of *Rhodopseudomonas sphaeroides* R-26: Localization of the binding site by chemical cross-linking and immunochemical studies, *Biochemistry 22*, 335−341.
23. Drepper, F., Dorlet, P., and Mathis, P. (1997) Cross-linked electron-transfer complex between cytochrome c_2 and the photosynthetic reaction center of *Rhodobacter sphaeroides*, *Biochemistry 36*, 1418−1427.
24. Hall, J., Zha, X., Durham, B., O'Brien, P., Vieira, B., Davis, D., Okamura, M., and Millett, F. (1987) Reaction of cytochromes c and c_2 with the *Rhodobacter sphaeroides* reaction center involves the heme crevice domain, *Biochemistry 26*, 4494−4500.
25. Miyashita, O., Onuchic, J. N., and Okamura, M. Y. (2003) Continuum electrostatic model for the binding of cytochrome c_2 to the photosynthetic reaction center from *Rhodobacter sphaeroides*, *Biochemistry 42*, 11651−11660.
26. Miyashita, O., Onuchic, J., and Okamura, M. (2004) Transition state and encounter complex for fast association of cytochrome c_2 with bacterial reaction center, *Proc. Natl. Acad. Sci. U.S.A. 101*, 16174−16179.
27. Wachtveitl, J., Farchaus, J., Mathis, P., and Oesterhelt, D. (1993) Tyrosine 162 of the photosynthetic reaction center l-subunit plays a critical role in the cytochrome c_2 mediated rereduction of the photooxidized bacteriochlorophyll dimer in *Rhodobacter sphaeroides*. 2. Quantitative kinetic analysis, *Biochemistry 32*, 10894−10904.
28. Paddock, M. L., Adelroth, P., Change, C., Abresch, E. C., Feher, G., and Okamura, M. Y. (2001) Identification of the proton pathway in bacterial reaction centers: Cooperation between Asp-M17 and Asp-L210 facilitates proton transfer to the secondary quinone (Q_B), *Biochemistry 40*, 6893−6902.
29. Donohue, T. J., McEvan, A. G., Van Doren, S., Crofts, A. R., and Kaplan, S. (1988) Phenotypic and genetic characterization of cytochrome c_2 deficient mutants of *Rhodobacter sphaeroides*, *Biochemistry 27*, 1918−1925.
30. Bartsch, R. (1978) in *The photosynthetic bacteria* (Clayton, R., and Sistrom, W., Eds.) pp 249−279, Plenum Press, New York.
31. Tetreault, M., Cusanovich, M., Meyer, T., Axelrod, H., and Okamura, M. (2002) Double mutant studies identify electrostatic interactions that are important for docking cytochrome c_2 onto the bacterial reaction center, *Biochemistry 41*, 5807−5815.
32. Serrano, L., Horovitz, A., Avron, B., Bycroft, M., and Fersht, A. (1990) Estimating the contribution of engineered surface electrostatic interactions to protein stability by using double-mutant cycles, *Biochemistry 29*, 9343−9352.
33. Hidalgo, P., and MacKinnon, R. (1995) Revealing the architecture of a K^+ channel pore through mutant cycles with a peptide inhibitor, *Science 268*, 307−310.
34. Brünger, A. T., Adams, P. D., Clore, G. M., DeLanod, W. L., Gros, P., Grosse-Kunstleve, R. W., Jiangf, J.-S., Kuszewski, J., Nilges, M., Pannu, N. S., Read, R. J., Rice, L. M., Simonson, T., and Warren, G. L. (1998) Crystallography & NMR system: A new software suite for macromolecular structure determination, *Acta Crystallogr. D54*, 905−921.
35. Mason, P., Neilson, G., Dempsey, C., Barnes, A., and Cruickshank, J. (2003) The hydration structure of guanidinium and thiocyanate ions: Implications for protein stability in aqueous solution, *Proc. Natl. Acad. Sci. U.S.A. 100*, 4557−4561.
36. Marcus, R. A., and Sutin, N. (1985) Electron transfer in chemistry and biology, *Biochim. Biophys. Acta 811*, 265−322.
37. Moser, C. C., Keske, J. M., Warnke, K., Farid, R. S., and Dutton, P. L. (1992) The nature of biological electron transfer, *Nature 355*, 796−802.
38. Beratan, D., Betts, J., and Onuchic, J. (1991) Protein electron transfer rates set by the bridging secondary and tertiary structure, *Science 252*, 1285−1288.
39. Aquino, A., Beroza, P., Beretan, D., and Onuchic, J. (1995) Docking and electron transfer between cytochrome c_2 and the photosynthetic reaction center, *Chem. Phys. 197*, 277−288.
40. Miyashita, O., Okamura, M. Y., and Onuchic, J. N. (2003) Theoretical understanding of the interprotein electron transfer between cytochrome c_2 and the photosynthetic reaction center, *J. Phys. Chem. B 107*, 1230−1241.
41. Hunte, C., Solmaz, S., and Lange, C. (2002) Electron transfer between yeast cytochrome bc_1 complex and cytochrome *c*: A structural analysis, *Biochim. Biophys. Acta 1555*, 21−28.
42. Gallivan, J., and Dougherty, D. (2000) A computational study of cation-π interactions versus salt bridges in aqueous media: Implications for protein engineering, *J. Am. Chem. Soc. 122*, 870−874.

BI050651D